Optimization of human walking for exoskeletal support

Wietse van Dijk, Herman van der Kooij
Department of Biomechanical Engineering
Delft University of Technology
Delft, The Netherlands
w.vandijk@tudelft.nl

Herman van der Kooij
Department of Biomechanical Engineering
MIRA, University of Twente
Enschede, The Netherlands

***Abstract*—It is hypothesized that healthy humans can reduce their energy expenditure during walking by wearing an exoskeleton. Exoskeletons are often designed for mechanical efficiency at joint level. This approach disregards the energy savings mechanisms in the human leg like bi-articular muscles and tendons. We use the muscle-reflex model to simulate the experiments by Cain et al. with an ankle exoskeleton actuated by a pneumatic muscle that supports plantarflexion. The muscle-reflex model predicts muscle activations and metabolic rate. The reflex-control parameters of the model were optimized for walking with and without support from an exoskeleton. The simulated exoskeleton uses either the EMG signal from the soleus muscle (proportional myoelectric control), or a footswitch to trigger the actuation of the pneumatic muscle. Cain et al. did find an experimental reduction in soleus muscle activation of 41.4 percent for the proportional myoelectric control and 13.0 percent for the footswitch control, where the optimization outcomes of simulated walking predicted a reduction of 42.8 percent and 25.9 percent respectively.**

Keywords—exoskeleton; walking; simulation; muscle; reflex; EMG; feedforward; feedback

I. INTRODUCTION

It is hypothesized that healthy humans can improve their walking performance by wearing an exoskeleton [1]. During the last decade the number of exoskeleton prototypes with the intention of doing this has greatly increased. Theoretical and experimental results give no conclusive answer on how humans can be most effectively supported during walking. One of the proposed strategies for multiple exoskeletons is to partially match the support with the torque patterns normally observed in human gait. Joint torques and powers are calculated using inverse dynamics. Exoskeletons that use this principle can be (quasi) passive systems [2-5], or active systems [6, 7]. The assumption made for the design of these systems is that if the gait kinematics and joint torques stay the same, the joint torques that the human has to provide will decrease, what will make the human walking effort, in mechanical terms, more efficient. However, in metabolic terms, these systems, as well as other systems [8, 9], have not or only slightly reduced energy expenditure during walking.

Manuscript received January 31, 2012. This work was supported by the EU within the EVRYON Collaborative Project (Evolving Morphologies for Human-Robot Symbiotic Interaction, Project FP7-ICT-2007-3-231451).

A problem with exoskeletons solely focusing on reducing joint torque or power is that they do not take into account the following effects: 1. Humans will adapt to the support, which results in different gait kinetics and kinematics [10] and 2. Tendons provide temporal energy storage and bi-articular muscles transfer energy between joints [5, 11]. We assume that due to this focus on mechanical efficiency, exoskeleton performance is often overestimated, and thereby leads to the poor results with reducing metabolic cost in exoskeletal walking studies.

More advanced walking models that take into account the human adaptation, and the effects of tendons and bi-articular muscles might better predict the effectiveness of an external support offered by an exoskeleton. This requires forward dynamical simulations to evaluate kinetic and kinematic adaptation effects and modeling of the musculoskeletal system to predict the effect of tendons and bi-articular muscles. Examples of such models are [12, 13]. The model we used in this study is the muscle-reflex model of [12]. The model is suitable for forward simulation of human walking, models musculoskeletal dynamics and control, and has a limited number of control parameters. The model has the flexibility to represent different gaits as has been shown by the optimization of the model for different walking speeds [14]. The model has been extended and optimized for walking and running in 3D [15], however this was done mainly for animation purposes and out of plane movements were not generated by a muscle model, but controlled by a PD-controller instead.

Aim of this study is to investigate if this model can be used for exoskeletal walking and if it can make predictions for the metabolic cost of walking. This requires the control parameters of the model to be optimized which is a highly non-linear optimization problem. A particle swarm optimization (PSO) is used to perform this optimization.

To test the model and the optimization two different types of external support that mimic the behavior of an exoskeleton were implemented in the walking simulation. The supports were modeled after the controllers used by [7] on a pneumatic ankle exoskeleton [16, 17].

The first implemented controller is the ankle torque feedforward (AFF) controller. The AFF controller plays back a

978-1-4673-6024-1/13/$31.00 ©2013 IEEE

fraction of a pre-recorded ankle torque pattern normally observed in human gait. This controller is modeled after the footswitch (FS) controller of [7] where the amount of support is controlled by a footswitch. A similar controller was also evaluated by [6]. The second implemented controller is the soleus activation feedback (SFB) controller. The SFB controller amplifies the soleus muscle activation signal generated by the muscle-reflex model. This controller is modeled after the proportional myoelectric controller (PM) of [7]. The PM controller measures the EMG of the soleus muscle and scales the support of the exoskeleton with this signal.

The study of [7] was selected since the results with this exoskeleton are well documented and different controllers have been applied on the same exoskeleton. In terms of mechanical power these two controllers offer a similar support, however the measured performance of the two controllers is different in terms of EMG, kinematics and adaptation time.

We hypothesize that the optimization of the muscle-reflex model for different exoskeletal supports can predict the experimental outcomes. Additionally the prediction of the metabolic cost [18] can be used to determine the metabolic advantage of the exoskeletal supports.

II. METHODS

A. Walking and exoskeleton model

The walking model which was used is the muscle-reflex model [12, 14]. The walking model consists of seven body segments with fourteen muscles. Each muscle has its own controllers that generate a muscle stimulation signal. Via the muscle dynamics this results in joint torques. The walking simulation is extended with an external support that acts around the ankle and mimics the support of the controllers implemented on the pneumatic ankle exoskeleton by [7]. Our support offers a torque directly at the ankle joint. Effects from the mass or actuator dynamics are not taken into account (Figure 1).

1) Ankle torque feed forward (AFF)

This controller plays back a fraction of the ankle torques (τ_{REF}) normally observed in human gait and that were acquired from an internal gait database. The ankle torques are defined as a function of the gait phase ($\phi(t)$). The gait phase is detected by an adaptive frequency oscillator that synchronizes the gait frequency with the right and the left hip angle [19]. Zero phase ($\phi(t) = 0$) is synchronized with the heel strike. The reference torques are scaled with a gain (G_{AFF}) and the control torque (τ_{AFF}) becomes:

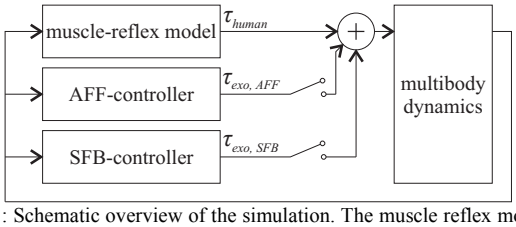

Figure 1: Schematic overview of the simulation. The muscle reflex model and exoskeleton controllers generate input torques for the multibody dynamics module that simultates the motion of the human body segments.

$$\tau_{AFF}(t) = G_{AFF}\,\tau_{REF}\left(\varphi(t)\right) \tag{0.1}$$

2) Soleus activation feedback (SFB)

This controller exerts an ankle torque (τ_{SFB}) that is proportional to the soleus activation (A_{SOL}) with a gain (G_{SFB}).

$$\tau_{SFB} = G_{SFB}\,A_{SOL} \tag{0.2}$$

The muscle activation signal of the muscle-reflex model is analogue to the rectified and filtered EMG signal measured in humans.

B. Simulations

The walking model has been implemented in a custom-made simulator for 2D rigid body dynamics for Matlab (Natick, Mass., USA). The simulator uses a fourth order Runge-Kutta integrator with a fixed time step of $5{\cdot}10^{-4}$ s. The software including the simulation results is available under a BSD license (dbl.tudelft.nl/exoskeleton/simulation/). Our simulations ran on 12 cores of a server with two Intel Xeon E5 2665 processors.

C. Optimization algorithm

The optimization algorithm which was used is a particle swarm optimization (PSO). A variant of the particle swarm optimization is used where each particle is influenced by its own best position over all the past iterations (x_{pbest}) and a local best position of the previous iteration ($x_{localbest}$). The local particles are determined by a ring topology, where each particle receives information of its n left and right neighbors. Additionally the velocity is damped with a factor ($\omega = 0.95$). The velocity (v) of particle j at iteration $k + 1$ is adjusted as follows:

$$v_{jk+1} = \omega v_{jk} + r_1(x_{pbest} - x_{jk}) + r_2(x_{socialbest} - x_{jk}) \tag{0.3}$$

where r is a random number between 0 and 1, and x_{jk} the position of particle j at iteration k. The positions of the particles are limited by x_{min}, x_{max} that are the bounds on the control parameters by [12]. The velocity of the particles v_{min}, v_{max} is limited as follows.

$$v_{\min} = -v_{\max} = 0.015\cdot\left(x_{\max} - x_{\min}\right) \tag{0.4}$$

1) Staged optimization

The PSO uses a staged optimization criterion. First the fitness of the first stage is calculated, if a desired fitness value is reached the particle moves to the next stage and the fitness of this next stage is calculated, until a final stage is reached. This can be interpreted as a constrained optimization problem where the stages are the constraints. In the optimization the following stages are used:

First stage is maximizing the simulation time close to its set maximum (t_{max} [s]). The simulation is terminated if the model falls. Maximizing the simulation time is in this case similar to ensuring that the model does not fall. The second criterion is a coarse matching of the walking speed. Third stage is the minimization of the standard deviation of the step time. This is a coarse measure for stability and it ensures a regular gait pattern. The fourth step is a fine matching of the gait speed.

The fifth, and final, step is the optimization of the product of: average muscle power, the RMS of the muscle activation averaged over the muscles, and average absolute ligament torques. The first two terms are introduced to optimize for an energy efficient gait pattern. The last term prevents for overstretching of ligaments and might be interpreted as a pain factor [14]. To determine the best particle out of a group of particles they are first sorted by their achieved stage and secondly on their fitness within that stage. The values choices for the fitness criteria are summarized in Table 1.

2) Muscle noise

To achieve more stable results muscle noise (e) was added to the model. For every stage and fitness evaluation by the PSO the simulation was repeated three times with different random initialized noise. Of the three acquired stages and fitness values the lowest was passed to the optimization algorithm. The noise is a piecewise polynomial fit through data points with random time intervals between 0.1 s and 0.2 s with random values between 0 and 1. The muscle stimulations (S) were adapted as follows:

$$S = (1 + 0.02e) \cdot S \tag{0.5}$$

D. Optimization experiments

Two optimization experiments were performed. The first optimization was used to optimize the initial conditions. The second optimization was walking with different types and levels of support. The settings of the PSO for the different experiments are given in Table 2. During all the experiments we optimized all the muscular control parameters of the reflex model. For the optimization of the initial conditions the lean angle of the torso (applied to the torso element and the shank of the stance leg), the angle of the swing leg and the speed of the swing leg were optimized as well, since the muscle-reflex model cannot start from every possible pose.

1) Optimizing initial conditions

The muscle-reflex model and the phase detection of the AFF controller require a few seconds of simulation before they reach steady state. Since the optimizations of supported walking require a long computation time, a series of optimizations were performed to optimize the initial conditions, so further simulations can start from a steady state walking cycle. These optimizations optimized walking without the support from the controllers. The maximal simulation time was 15 seconds. To check the convergence of the results the optimization was repeated five times. The state of the walker at t = 10 s of the optimization with the best fitness was used as the initial state for the further experiments. The computation time for this experiment was two hours per repetition.

TABLE 1: DYNAMIC PROPERTIES LOPES

Stage	Fitness	Criterion next stage
1	Simulation time [s]	> t_{max} - 0.01s
2	abs(Speed – Desired speed) [m/s]	< 0.5m/s
3	std(Step time) [s]	< 0.05s
4	abs(Speed – Desired speed) [m/s]	< 0.1m/s
5	Average muscle power [W/kg] x muscle activation RMS [] x average absolute ligament torques [Nm/kg]	--

2) Optimizing supported walking

After the initial conditions were determined walking with and without the different controllers was optimized. We optimized for different walking conditions: walking with SFB controller, walking with AFF controller, and walking without support. The amount of support was gradually increased over eight optimizations, indicated by the optimization step (i_{step}). This was done to obtain results for different levels of support. For the SFB controller the gain (G_{SFB}) is:

$$G_{SFB} = (30 \cdot i_{step} - 1) \quad i_{step} = 1..8 \tag{0.6}$$

For the AFF controller the gain (G_{AFF}) is a function of the body mass (m) and the step:

$$G_{AFF} = 0.06 \cdot m \cdot (i_{step} - 1) \quad i = 1..8 \tag{0.7}$$

For the normal walking there is no change in the support. Still the same multistep approach was chosen for walking without support, so all optimizations have a similar number of iterations of the PSO.

The initial population of each optimization step, except for the first optimization step, is a random population around the best particle from the previous step. The position of each new particle is seeded within +/-15% of the search space size around the best particle of the previous step (respecting the bounds on the search space). In order to evaluate the convergence of the results the experiment was repeated ten times. The computation time for this experiment was approximately twenty hours per repetition.

E. Data processing

For each optimization result an average step was calculated from the last five steps of each simulation. The amount of support was characterized by the maximal support power in an average step. For the experimental results by [7] this was 1.23 and 1.18 Wkg^{-1} for the FS and PM controller respectively. The average of 1.20 Wkg^{-1} was used as the target support power for our optimization. From the different optimization steps, the results from the optimization step where the maximal support powers were closest to this target were selected.

Three different energy related measures for the evaluation of walking performance are used. 1. Average absolute joint power. The average was taken over the time and summed over the joints. 2. Average muscle power. This is the power from the contractile element of the muscle averaged over time and summed over the muscles. 3. Estimated metabolic cost. The estimated metabolic cost using the model of [18] takes into account the muscle activation and maintenance heat, the shortening and lengthening heat, and the mechanical work. All these measures are normalized with the body weight. Results for the different controllers are compared to each other.

TABLE 2: SETTINGS USED FOR THE PSO

	Initial conditions	Supported walking	
step	--	1th step	2nd to 8th
Population	50	60	40
Population 1st iteration	100	120	80
Iterations	60	75	50
Particle neighbours (n)	2	7	5

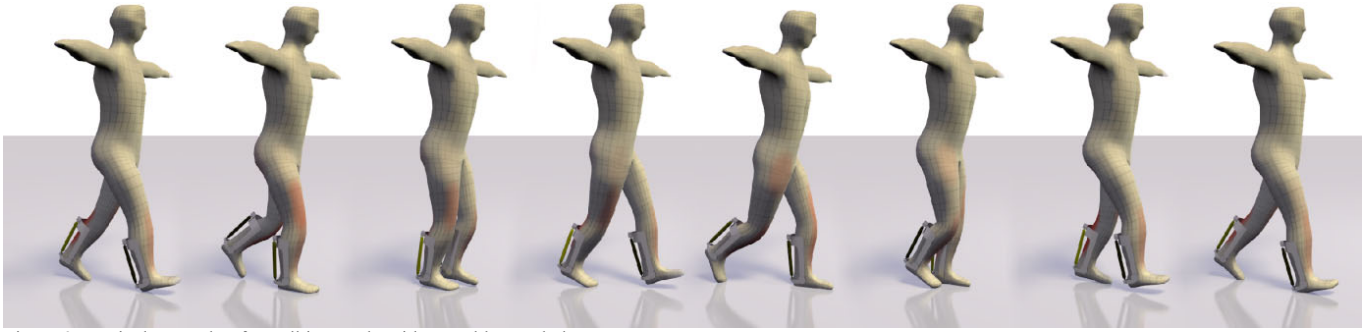

Figure 2: Typical example of a walking cycle with an ankle exoskeleton.

TABLE 3: DIFFERENT MEASURES FOR THE HUMAN ENERGY EXPENDITURE

	All joints			**Ankle only**		
	No support	***SFB***	***AFF***	***No support***	***SFB***	***AFF***
Metabolic rate [Wkg^{-1}]	2.82 (0.05)	2.82(0.13)	2.63(0.13)*	0.486 (0.058)*	0.378 (0.024)*	0.340(0.051)*
Muscle power [Wkg^{-1}]	1.12 (0.06)	1.23 (0.07)*	1.12 (0.06)	0.157(0.008)*	0.147 (0.014)*	0.149 (0.010)*
Joint power [Wkg^{-1}]	2.34 (0.15)	2.27 (0.12)	2.17(0.12)	0.656 (0.032)*	0.413 (0.033)*	0.494 (0.067)*

Results are shown for all joints together and for the ankle only. The muscle energy expenditure and the muscle power for the ankle only was based in data from, the soleus, tibialis anterior and gastrocnemius muscles. Values between brackets denote standard deviations over the repetitions of the experiment. * denotes a significant difference between the results with controller from results for unsupported walking (single sided ANOVA, $p < 0.05$)

Statistics are performed with a single sided ANOVA-test over all the results from the different repetitions of the experiment.

III. RESULTS

A. Optimization

During all optimizations on average 31.9% and at least 7.5% of the particles reached the final stage of the five fitness stages in the last iteration of the optimization. This means that for all optimizations, solutions were found that fulfilled the criteria for optimization stages one to four. A typical example of a walking cycle that was optimized is shown in Figure 2. A selection of the results with animations is placed online (dbl.tudelft.nl/exoskeleton/simulation/). For both controllers the simulation step where the maximal support power (P_{max}) was closest to the maximal support power of [7] was selected (Figure 3). For the SFB controller this was the fourth optimization step (G_{SFB} = 90 Nm, P_{max} = 1.18 W/kg) and the fifth optimization step for the AFF controller (G_{AFF} = 0.24 $Nmkg^{-1}$, P_{max} = 1.04 Wkg^{-1}). Further results will describe the data acquired from these optimization steps.

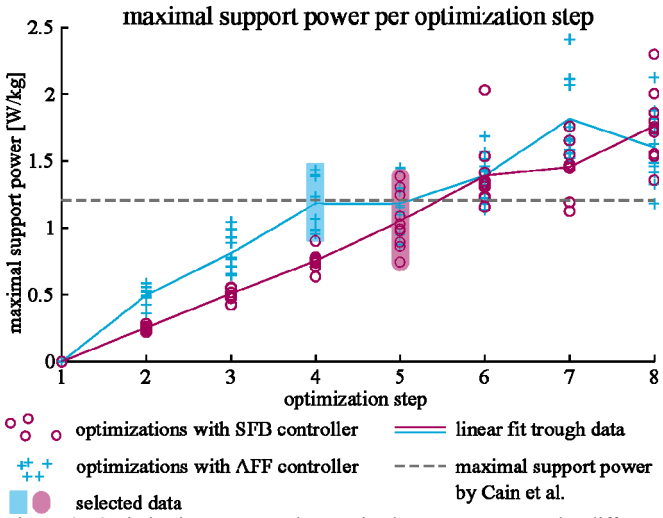

Figure 3: Optimization step vs. the maximal support power. The different markers for each optimization step represent the data acquired from the different repetitions of the experiment.

B. Support vs. joint power, muscle power and energy expenditure

Different energy measures were calculated from the results. The average absolute joint power, the average power of the contractile elements in the muscle, and the estimated metabolic cost calculated using the model of [18] are given in Table 3. The results are given for all the joints together and for the ankle only.

C. Ankle kinematics and kinetics

The average ankle angle, ankle torque, and ankle power are shown in Figure 4. The ankle kinematics for walking with and without the support are compared with the cross correlation coefficient. For the SFB controller the correlation with unsupported walking is 0.98. For the AFF controller the correlation with unsupported walking is 0.99.

D. Support work vs. muscle activation

The muscle activations for the different controllers are compared in Figure 5. Significant decreases of 42.8% and 25.9% in soleus activation were found for the SFB controller and AFF controller respectively (experimentally found reductions were 41.4% and 13.0%). For the SFB controller we found a significant increase for the tibialis anterior and the gluteus muscles of respectively 16.0% and 5.4%, in the experiment by Cain et al. these changes were not significant. For the AFF controller we found a significant reduction of 37.9% and 10.0% in respectively the activation of the gastrocnemius and vastus muscles. Cain et al found a decrease in the gastrocnemius muscles of 27.7% and 9.77% for the PM and FS controller respectively.

IV. Discussion

A. Optimization

The used optimization algorithm was able to find stable gait patterns for the different controllers and the different levels of support. This is a first indication that the muscle-reflex model is able to simulate walking with exoskeletons or orthoses.

B. Gait kinematics

The different conditions led to very similar gait kinematics for the ankle. Cain et al. have shown in their experiments that the initial gait kinematics showed more plantar flexion and converged to a gait pattern closer to that of normal walking. This adaptation process cannot be captured with the optimizations. The PM controller of Cain et al. and the results for the SFB controller both show a gait pattern very similar to that of unsupported walking. Cain et al. showed that the gait kinematics of the footswitch controller even after convergence showed large deviations from a normal gait pattern, where this was not observed with the AFF controller we evaluated. The FS controller of Cain et al. produces a weaker resemblance to a normal ankle torque signal since it is controlled by an on/off signal coming from the footswitch, which might have contributed to the different gait pattern.

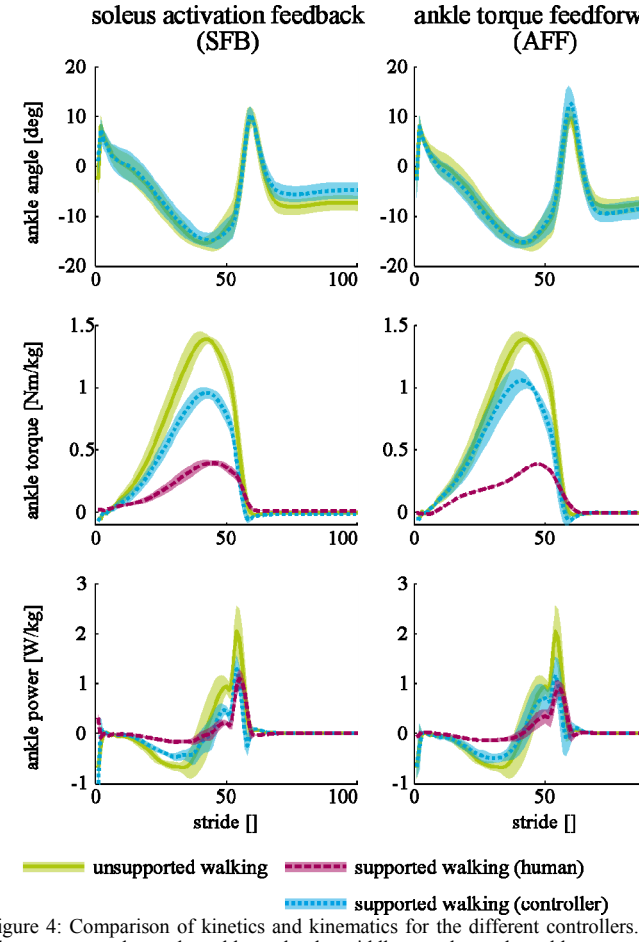

Figure 4: Comparison of kinetics and kinematics for the different controllers. The upper row shows the ankle angle, the middle row shows the ankle torque, the bottom row shows the ankle power. Plantarflexion is positive.

C. Muscle activation

The studies from Cain showed that both controllers have the biggest effect on the activity of the soleus muscle, which was confirmed by our simulation results. We also found a big reduction in gastrocnemius activation for the AFF controller that was not found by Cain et al. It should be noted that the standard deviation in the gastrocnemius activation over the

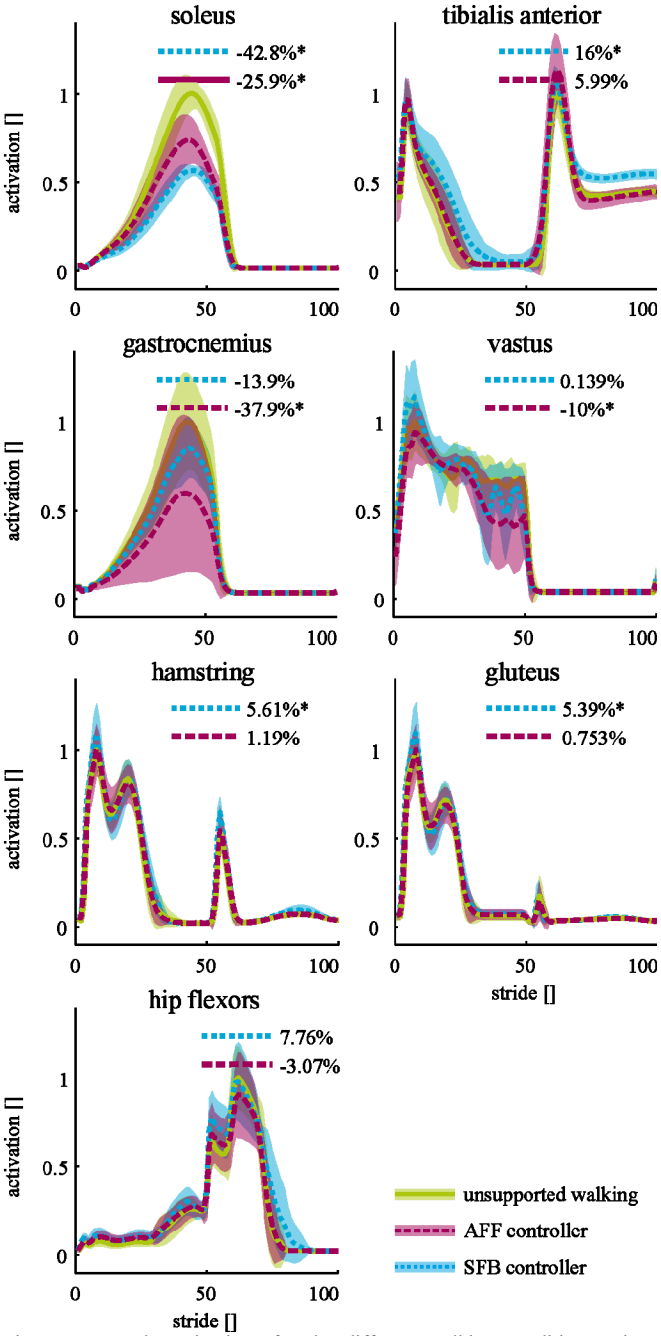

Figure 5: Muscle activations for the different walking conditions. Lines denote the mean, shaded areas denote the standard deviations taken over the last five steps of the different optimizations. The data is normalized to the walking condition without support. The percentages show the difference in RMS between no support and walking with the controllers. * denotes a significant difference between the results with controller from results without controller (single sided ANOVA, $p < 0.05$)

different repetitions of the optimization was large. Cain et al. did find a significant reduction in gastrocnemius EMG for the SFB controller that we did not find, but in another study with the same controller by [17] this reduction was not found. Additionally we found numerous smaller differences that were significant, but not reported in the experimental study. These effects are small and they might not be noticed in experiments due to inter-subject differences.

D. Energy expenditure

Of the different energy measures (absolute joint power, muscle power, and metabolic rate) evaluated over all the joints, only the metabolic rate for the AFF controller decreases significantly. A possible explanation might be that reductions in energy expenditure at the ankle are counteracted by increases in energy expenditure at the knee and hip. Additionally the muscle-reflex model tends to overestimate the hip and knee power, making the relative contribution of the ankle smaller. To rule out these effects the ankle was also evaluated in isolation. For the ankle alone all performance measures predicted a decrease in energy consumption. Experimental data with the proportional feedback controller showed reductions in metabolic rate of 0.39 Wkg^{-1} (3.39 Wkg^{-1} with the unpowered device, 3.00 Wkg^{-1} with the powered device) [20]. The simulations with the SFB controller only predicted savings of 0.108 Wkg^{-1}. The prediction of the reduction in muscle power showed the smallest gain in energy efficiency by the controllers. The predictions of reductions in joint power and metabolic rate were on a comparable scale. For the AFF controller the relative reduction in metabolic rate was larger, for the SFB the relative reduction in joint power was larger.

Our research has some limitations that might be addressed in future research. Although the muscle reflex model has a good resemblance of human walking the model is not validated. Our research considers only the torque exerted by the exoskeleton. The mass of the exoskeleton was not taken into account. However, added mass to the leg does have a significant influence on the walking performance [9, 20, 21].

V. CONCLUSION

We have shown that the muscle-reflex model adapts to an external support. Muscle activation patterns showed similar changes as the experimental recordings of EMG when an ankle support is provided. In general, changes in muscle activation and metabolism predicted by the simulation were lower than the observed changes in the experiment. For this study we only used experimental data from one exoskeleton as reference. Based on this reference we conclude that the simulations give a conservative estimation of the reduction in human energy expenditure. Estimated metabolic rate and joint power showed similar reductions. Our hypothesis that reductions in estimated metabolic rate would be lower than reductions in joint power was not confirmed. Still the estimated metabolic rate is a physiologically sounder estimate of the human energy expenditure than absolute joint power.

VI. REFERENCES

[1] D. P. Ferris, G. S. Sawicki, and M. A. Daley, "A physiologist's perspective on robotic exoskeletons for human locomotion," International journal of HR: humanoid robotics, vol. 4, pp. 507-528, 2007.

[2] A. J. van den Bogert, "Exotendons for assistance of human locomotion," BioMedical Engineering OnLine, vol. 2, p. 17, 2003.

[3] W. van Dijk, H. van der Kooij, and E. Hekman, "A passive exoskeleton with artificial tendons: Design and experimental evaluation," in Rehabilitation Robotics (ICORR), 2011 IEEE International Conference on, 2011, pp. 1-6.

[4] C. Walsh, K. Endo, and H. Herr, "A quasi-passive leg exoskeleton for load-carrying augmentation," International Journal of Humanoid Robotics, vol. 4, pp. 487-506, 2007.

[5] M. B. Wiggin, G. S. Sawicki, and S. H. Collins, "An exoskeleton using controlled energy storage and release to aid ankle propulsion," in Rehabilitation Robotics (ICORR), 2011 IEEE International Conference on, 2011, pp. 1-5.

[6] J. A. Norris, K. P. Granata, M. R. Mitros, E. M. Byrne, and A. P. Marsh, "Effect of augmented plantarflexion power on preferred walking speed and economy in young and older adults," Gait & Posture, vol. 25, p. 620, 2007.

[7] S. M. Cain, K. E. Gordon, and D. P. Ferris, "Journal of NeuroEngineering and Rehabilitation," Journal of NeuroEngineering and rehabilitation, vol. 4, p. 48, 2007.

[8] H. Herr, "Exoskeletons and orthoses: classification, design challenges and future directions," Journal of NeuroEngineering and rehabilitation, vol. 6, p. 21, 2009.

[9] P. Malcolm, W. Derave, S. Galle, and D. De Clercq, "A Simple Exoskeleton That Assists Plantarflexion Can Reduce the Metabolic Cost of Human Walking," PLoS ONE, vol. 8, p. e56137, 2013.

[10] P.-C. Kao, C. L. Lewis, and D. P. Ferris, "Invariant ankle moment patterns when walking with and without a robotic ankle exoskeleton," Journal of Biomechanics, vol. 43, pp. 203-209, 2010.

[11] M. Ishikawa, P. V. Komi, M. J. Grey, V. Lepola, and G. P. Bruggemann, "Muscle-tendon interaction and elastic energy usage in human walking," Journal of Applied Physiology, vol. 99, pp. 603-608, 2005.

[12] H. Geyer and H. Herr, "A muscle-reflex model that encodes principles of legged mechanics produces human walking dynamics and muscle activities," Neural Systems and Rehabilitation Engineering, IEEE Transactions on, vol. 18, pp. 263-273, 2010.

[13] A. J. van den Bogert, D. Blana, and D. Heinrich, "Implicit methods for efficient musculoskeletal simulation and optimal control," Procedia IUTAM, vol. 2, pp. 297-316, 2011.

[14] S. Seungmoon and H. Geyer, "Regulating speed and generating large speed transitions in a neuromuscular human walking model," in Robotics and Automation (ICRA), 2012 IEEE International Conference on, 2012, pp. 511-516.

[15] J. M. Wang, S. R. Hamner, S. L. Delp, and V. Koltun, "Optimizing locomotion controllers using biologically-based actuators and objectives," ACM Transactions on Graphics (TOG), vol. 31, p. 25, 2012.

[16] D. P. Ferris, K. E. Gordona, and G. S. Sawickia, "An improved powered ankle–foot orthosis using proportional myoelectric control," Gait & Posture, vol. 23, pp. 425–428, 2005.

[17] K. E. Gordon, G. S. Sawicki, and D. P. Ferris, "Mechanical performance of artificial pneumatic muscles to power an ankle-foot orthosis," Journal of Biomechanics, vol. 39, pp. 1832-1841, 2006.

[18] B. R. Umberger, K. G. M. Gerritsen, and P. E. Martin, "A model of human muscle energy expenditure," Computer methods in biomechanics and biomedical engineering, vol. 6, pp. 99-112, 2003.

[19] L. Righetti, J. Buchli, and A. J. Ijspeert, "Dynamic Hebbian learning in adaptive frequency oscillators," Physica D: Nonlinear Phenomena, vol. 216, pp. 269-281, 2006.

[20] G. S. Sawicki and D. P. Ferris, "Powered ankle exoskeletons reveal the metabolic cost of plantar flexor mechanical work during walking with longer steps at constant step frequency," Journal of Experimental Biology, vol. 212, pp. 21-31, 2009.

[21] R. C. Browning, J. R. Modica, R. Kram, and A. Goswami, "The effects of adding mass to the legs on the energetics and biomechanics of walking," Med Sci Sports Exerc., vol. 39, pp. 515-25., 2007 Mar 2007.